

Interconversion between Discrete and a Chain of Nanocages: Self-Assembly via a Solvent-Driven, Dimension-Augmentation Strategy

Tian-Fu Liu, Ying-Pin Chen, Andrey A. Yakovenko, and Hong-Cai Zhou*

Department of Chemistry, Texas A&M University, PO Box 30012, College Station, Texas 77842, United States

S Supporting Information

ABSTRACT: Using a ligand bearing a bulky hydrophobic group, a “shish kabob” of nanocages, has been assembled through either a one-fell-swoop or a step-by-step procedure by varying the dielectric constant of the assembly mixture. A hydrophobic solvent breaks down the chain to discrete nanocages, while a hydrophilic solvent reverses the procedure. Although the shish kabob of nanocages has exactly the same chemical composition and even the same Archimedean-solid structure as those of its discrete analogue, its gas-adsorption capacity is remarkably improved because assembly of a chain exposes the internal surface of an individual cage. This dimension-augmentation strategy may have general implications in the preparation of porous materials.

Metal–organic polyhedra (MOPs), also known as coordination nanocages, have attracted great interest in the past two decades.¹ Different from metal–organic frameworks (MOFs), MOPs are discrete metal–organic molecular assemblies with well-defined cavities. Their unique structural and chemical properties make them ideal candidates for many applications, such as catalysis, drug delivery, and molecular capsulation.² Significant progress has been made in rational design of MOPs. Some design strategies including edge-directed and face-directed self-assembly,³ symmetry interaction model, and molecular library approach,⁴ as well as bridging ligand-substitution strategy,⁵ have been systematically investigated. However, compared with MOFs, one of the daunting challenges for MOPs is their very limited gas uptake, which severely impairs its application potential. It is mainly because MOPs, as discrete molecular assemblies, form crystals through packing and often lose crystallinity upon activation. Even though most of the MOPs may have internal cavities, the molecular cages usually rearrange after solvent removal. Therefore, the array of MOPs loses channel continuity in solids, which hampers the diffusion of gas molecules. Hence, finding ways of fixing the relative position of nanocages to construct continuous open channels would dramatically improve the effectiveness of these nanocages in gas storage and other applications.

In the last five years, our laboratory has utilized a number of carboxylate ligands with bulky hydrophobic groups to make a series of mesh-adjustable molecular sieves, whose mesh size can be tuned by temperature changes.⁶ The hydrophilic ends (carboxylate groups) bind metal clusters to afford two-dimensional layers, and the bulky hydrophobic groups of

adjacent layers are mutually interdigitated to form adjustable chambers with dynamic sorption properties. The interdigitation of the bulky hydrophobic groups plays a vital role for the novel structures and the unique temperature-responsive feature. It is interesting to contemplate whether the interdigitation could happen between adjacent nanocages. In this case, it would represent an effective route to prevent the rearrangement of discrete cages upon activation and consequently improve structural stability and maintain channel continuity in solids.

With this motivation, we undertook the synthesis of MOPs using ligands with bulky hydrophobic groups. A surfactant-like amphiphilic ligand, 5-((triisopropylsilyl)ethynyl) isophthalate (TEI), consisting of a bulky hydrophobic end and two hydrophilic carboxylate functional groups (Figure 1a), was

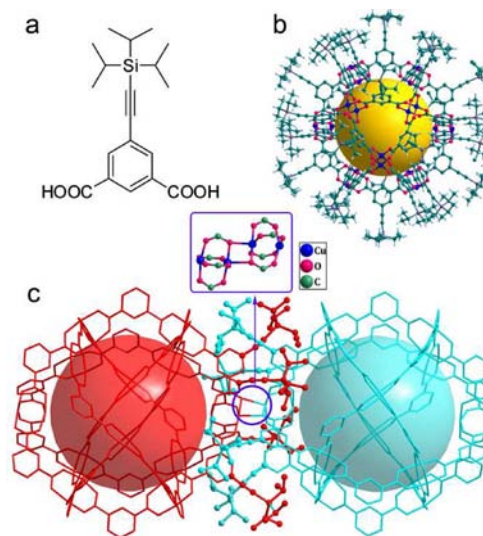


Figure 1. (a) Protonated TEI. (b) Crystal structure of **1**. (c) Crystal structure of **2**, some of the triisopropylsilyl-ethynyl groups being omitted for clarity. (inset) The coordination mode of carboxylate groups linking neighboring cages.

adopted for this purpose. Combining TEI and Cu(II), we reported a micelle-like cuboctahedral nanocage (denoted as **1** hereafter, Figure 1b) with 24 triisopropylsilyl (TIPS) groups on the exterior.⁷ Herein, with the same ligand and metal source, we present a novel nanocage-based chain structure in which the bulky groups of the adjacent cuboctahedral cages are mutually

Received: June 28, 2012

Published: October 8, 2012

interdigitated, and two of the metal vertices are further linked by two oxygen atoms from neighboring cages to form a shish kabob of nanocages (denoted as **2** hereafter, Figure 1c). In general, in a hydrophobic solution, the hydrophobic ends of a surfactant tend to have more contact with the solvent, whereas the hydrophilic ends try to have less contact with the solvent; this is the driving force for micelle (or inverse micelle) formation.⁸ As expected, a micelle-like compound, nanocage **1** was obtained in a hydrophobic mixture of solvents (benzene:methanol = 19:1). As shown in Figure 1b, **1** is a coordination nanocage assembled from 12 $\text{Cu}_2(\text{CO}_2)_4$ paddlewheel motifs and 24 isophthalate bridging ligands to give a cuboctahedron. It has 8 triangular (ca. 8 Å) and 6 square (ca. 12 Å) windows with an enclosed void with a diameter of ca. 15 Å. Remarkably, by employing the same starting materials but in a hydrophilic mixture of solvents (DMF:water = 1:2), the exact same cuboctahedral nanocages were assembled except the mutual interdigitation of the TIPS groups from adjacent cages, giving rise to a shish kabob of cuboctahedra (Figure 1c). This kind of interdigitation was also observed between the adjacent chains as shown in Figure S3 in Supporting Information (SI). A close examination of the structure revealed that the two closest Cu(II) ions from two adjacent cages were linked through two carboxylate group in a bidentate-bridging mode with Cu–O bond lengths of 2.272(11) and 2.426(14) Å, respectively (Figure 1, inset). Presumably the hydrophobic effect is the driving force behind the formation of **2**. It is well-known that there exists unusually strong attractions between hydrophobic groups in a hydrophilic environment.⁹ Evidently, by adhering to each other, hydrophobic groups can minimize their contact with a hydrophilic environment. Such behavior was also widely observed in natural processes, such as protein folding and membrane formation.¹⁰ In the current case, the hydrophobic effect forces the coordination cages to aggregate and leads to the formation of two Cu–O bonds between a pair of adjacent cages, thereby extending the structure to a 1D chain.

Keeping these considerations in mind, we set out to investigate whether changing the dielectric constant of the solvent mixture can drive structural transformation between **2** and **1**. In the center of Figure 2, an as-prepared sample of **2** was

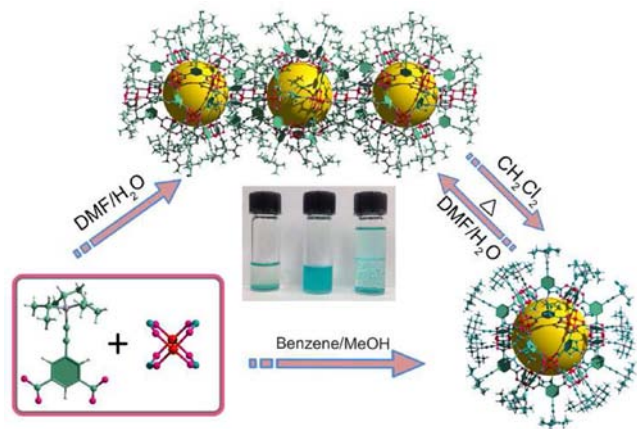


Figure 2. Illustrations of the self-assembly processes and interconversion of cuboctahedral cages, **1** (bottom-right), and the 1D chain, **2** (top). Bottom-left, a TEI ligand and a dicopper paddlewheel. Center, the as-synthesized **2** in mother liquid (left); dissolving **2** in CH_2Cl_2 (middle) leads to the formation of **1**; and recrystallization in $\text{CH}_2\text{Cl}_2/\text{DMF}$ (right) gives teal crystals of **1**.

shown together with the mother liquor (Figure 2, center, left). When suspended in CH_2Cl_2 , **2** dissolved quickly to give a teal solution (Figure 2, center, middle). Matrix-assisted laser desorption/ionization time-of-flight (MALDI-TOF) mass spectrometry reveals a high-intensity peak of m/z 9902.69, which corresponds to a formula of $\text{Cu}_{24}(\text{TEI})_{24}\cdot 6\text{H}_2\text{O}$ (**1**). Teal crystals of **1** were obtained when the CH_2Cl_2 solution was layered with DMF, and the mixture was allowed to stay (Figure 2, center, right). The subsequent powder X-ray diffraction (PXRD) studies further confirmed the complete conversion of **2** to **1** (Figure S5).

The dissociation of the 1D chain into discrete nanocages presumably happened due to a solvation effect of methylene chloride. Furthermore, a sample of **1** was immersed in 1.5 mL DMF/ H_2O (with a volume ratio of 1:2, the same as that for the synthesis of **2**) in a 2 mL vial, which was subsequently kept at 85 °C for three days, after which PXRD patterns were collected, indicating a complete conversion of **1** to **2**. These solvent-driven structural transformations further confirm the hydrophobic effect as a driving force in the formation of the shish kabob of nanocages. For the transformation from **2** to **1**, the solvation of the hydrophobic nanocages by methylene chloride is an exothermic procedure, which compensates for the energy needs of breaking the intercage Cu–O bonds. In contrast, when the hydrophobic **1** was subject to heating in a hydrophilic solvent, the hydrophobic effect made the cages aggregate into a 1D chain with the formation of intercage Cu–O bonds, reducing the hydrophobic–hydrophilic contact.

This type of stimuli-responsive synthetic strategy has been applied in the self-assembly processes of other structures. For example, some amphiphilic block copolymers can self-assemble into micelles in response to environmental changes, such as solvent, temperature, and pH.¹¹ Herein, the aggregation of nanocages, mimicking the stimuli responsiveness in protein folding and membrane formation, was observed in MOPs for the first time. It also provides us a new synthetic strategy to achieve higher dimensional self-assembled arrays.

As anticipated, the interdigitation and the Cu–O bonds between neighboring cages effectively prevent the rearrangement of cages in the solid state upon activation and preserve the structural integrity of **2**, which are demonstrated by the much-improved porosity and gas sorption capacities compared with **1** (Table 1). The total potential solvent-accessible volume

Table 1. Adsorption Capacities ($\text{cm}^3\cdot\text{g}^{-1}$) of **1** and **2** for N_2 , O_2 , H_2 (at 77 K), CO_2 , and CH_4 (at 195 K)

compound	N_2	O_2	H_2	Ar	CO_2	CH_4
1	5	8	41	6	71	23
2	214	216	115	160	169	82

is 36% estimated by using the PLATON routine.¹² N_2 adsorption study on an activated sample of **2** revealed a BET surface area of $739 \text{ m}^2\cdot\text{g}^{-1}$ (Langmuir $843 \text{ m}^2\cdot\text{g}^{-1}$), among the highest reported for MOPs to date.¹³ It is worth noting that **2** has a pore volume of $0.292 \text{ cm}^3\cdot\text{g}^{-1}$ estimated based on sorption isotherms, comparable to that estimated by using the PLATON routine ($0.317 \text{ cm}^3\cdot\text{g}^{-1}$).¹² Moreover, **2** retains its porosity and crystallinity after many adsorption–desorption cycles. These findings demonstrate the high stability and permanent porosity of **2**.

The gas sorption isotherms of H_2 , CO_2 , and CH_4 for **2** all exhibit type I behavior, and all the gas uptakes are significantly

higher than those of **1** (Figure 3 and Table 1). Meanwhile, the N_2 , O_2 , and Ar sorption isotherms of **2** exhibit hysteric

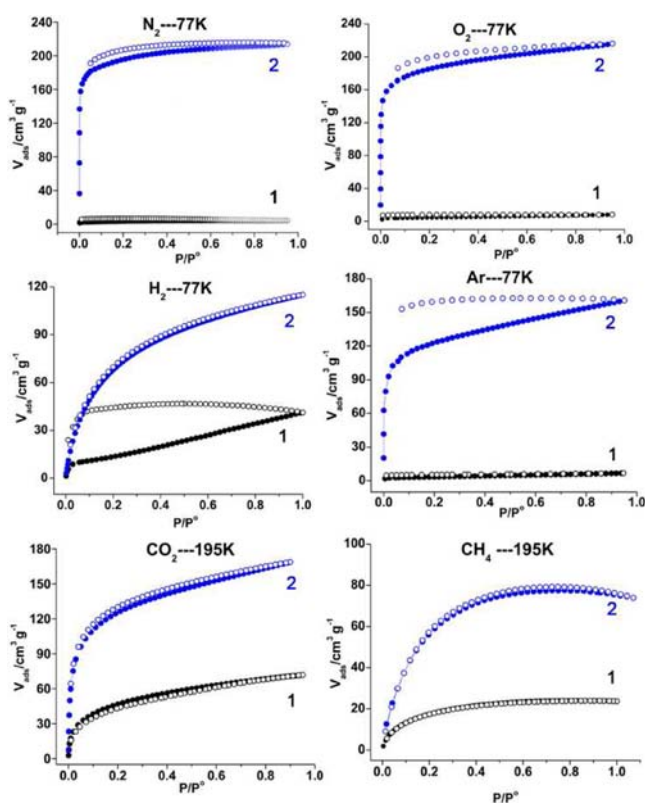


Figure 3. The sorption isotherms of N_2 , O_2 , H_2 , Ar at 77 K, and CO_2 , CH_4 at 195 K, for **1** and **2** (equilibrium time is 5 s for both **1** and **2**).

behavior on the desorption-branch with an equilibrium time of 5 s during the measurement. To explore the cause of the hysteresis, we measured Ar isotherms in different conditions. The results indicated that the hysteresis loop was effectively decreased when raising the adsorption temperature from 77 to 87 K. A similar phenomenon was observed when adsorbate was introduced slowly into the pore by extending the equilibrium time. However, the hysteresis cannot be completely eliminated even when the equilibrium time was extended to 20 s (Figure S9). This type of sorption behavior most likely arises from a porous structure with small openings connecting large cavities, leading to the trapping of relatively large gas molecules at low temperatures.⁷ At higher temperatures, such as in the cases of 195 and 87 K or when the gas molecules are smaller, as in the case of hydrogen albeit at 77 K, the hysteresis vanishes, reminiscent of the adsorption behavior of the mesh-adjustable molecule sieves.^{6,7} This phenomenon corroborates well with the crystal structure, in which the nanocage possesses two types of openings that are much smaller than the size of the cavity. More importantly, the enhancement of gas adsorption capacity of various gases of up to 43 folds (for N_2) implies the power of dimension augmentation. In going from 0D to 1D, the internal surfaces of the molecular cages became more exposed. It is tempting to extrapolate this dimension augmentation strategy further to 2D and 3D; this work is currently under way in our laboratory.

In conclusion, we have presented a shish kabob of nanocages in which the discrete nanocages are mutually interdigitated by bulky hydrophobic groups and linked by Cu–O bonds to form

a nanocage chain structure. The hydrophobic bulky group plays a vital role in the formation of the novel structure. By changing the hydrophobicity/hydrophilicity of the solvent mixture for assembly, reversible transformation between the shish kabob (**2**) and discrete nanocages (**1**) can be achieved. The solvent-responsive process mimics the stimuli responsiveness of natural processes, such as micelle formation, protein folding, and membrane construction. More importantly, the stability and gas-adsorption capacity of **2** were greatly improved compared with those of **1**. This provides a strategy for the assembly of coordination nanocages with higher stability and permanent porosity, which may have general implications in the control of assembly processes through dimension augmentation.

■ ASSOCIATED CONTENT

Supporting Information

Full details for sample preparation and characterization results, and crystallographic data (CIF). This material is available free of charge via the Internet at <http://pubs.acs.org>.

■ AUTHOR INFORMATION

Corresponding Author

zhou@mail.chem.tamu.edu

Notes

The authors declare no competing financial interest.

■ ACKNOWLEDGMENTS

This work was supported by the U.S. Department of Energy (DE-SC0001015 and DE-AR0000073), the National Science Foundation (CBET-0930079), and the Welch Foundation (A-1725). We are thankful to Dr. Joseph H. Reibenspies and Dr. George. M. Sheldrick to providing access to SHELXL 2012 software.

■ REFERENCES

- (a) Eddaoudi, M.; Kim, J.; Wachter, J. B.; Chae, H. K.; O'Keeffe, M.; Yaghi, O. M. *J. Am. Chem. Soc.* **2001**, *123*, 4368. (b) Ghosh, K.; Hu, J.; White, H. S.; Stang, P. J. *J. Am. Chem. Soc.* **2009**, *131*, 6695. (c) Chen, C.; Zhang, J.; Su, C. *Eur. J. Inorg. Chem.* **2007**, 2997. (d) Lim, S. H.; Su, Y.; Cohen, S. M. *Angew. Chem., Int. Ed.* **2012**, *51*, 5106. (e) Liu, M.; Liao, W.; Hu, C.; Du, S.; Zhang, H. *Angew. Chem., Int. Ed.* **2012**, *51*, 1585. (f) Sun, Q.-F.; Sato, S.; Fujita, M. *Nature Chem.* **2012**, *4*, 330.
- (a) Férey, G.; Mellot-Draznieks, C.; Serre, C.; Millange, F.; Dutour, J.; Surblé, S.; Margiolaki, I. *Science* **2005**, *309*, 2040. (b) Sun, Q.-F.; Iwasa, J.; Ogawa, D.; Ishido, Y.; Sato, S.; Ozeki, T.; Sei, Y.; Yamaguchi, K.; Fujita, M. *Science* **2010**, *328*, 1144. (c) Abrahams, B. F.; FitzGerald, N. J.; Robson, R. *Angew. Chem., Int. Ed.* **2010**, *49*, 2896. (d) Wang, Z. J.; Brown, C. J.; Bergman, R. G.; Raymond, K. N.; Toste, F. D. *J. Am. Chem. Soc.* **2011**, *133*, 7358. (e) Mal, P.; Breiner, B.; Rissanen, K.; Nitschke, J. R. *Science* **2009**, *324*, 1697. (f) McManus, G. J.; Wang, Z.; Zaworotko, M. J. *Cryst. Growth Des.* **2004**, *4*, 11.
- (a) Seidel, S. R.; Stang, P. J. *Acc. Chem. Res.* **2002**, *35*, 972.
- (a) Leininger, S.; Olenyuk, B.; Stang, P. J. *Chem. Rev.* **2000**, *100*, 853. (b) Tranchemontagne, D. J.; Ni, Z.; O'Keeffe, M.; Yaghi, O. M. *Angew. Chem., Int. Ed.* **2008**, *47*, 5136.
- Li, J.-R.; Zhou, H.-C. *Nat. Chem.* **2010**, *2*, 893.
- (a) Ma, S.; Sun, D.; Wang, X.-S.; Zhou, H.-C. *Angew. Chem., Int. Ed.* **2007**, *46*, 2458. (b) Ma, S.; Sun, D.; Yuan, D.; Wang, X.-S.; Zhou, H.-C. *J. Am. Chem. Soc.* **2009**, *131*, 6445.
- Zhao, D.; Yuan, D.; Krishna, R.; van Baten, J. M.; Zhou, H.-C. *Chem. Commun.* **2010**, *46*, 7352.
- (a) Nagarajan, R.; Ganesh, K. J. *Chem. Phys.* **1989**, *90*, 5843. (b) Alawi, S. M.; Akhter, M. S. J. *Mol. Liquids* **2011**, *160*, 63.

(9) (a) Southall, N. T.; Dill, K. A.; Haymet, A. D. J. *J. Phys. Chem. B* **2002**, *106*, 521. (b) Meyer, E. E.; Rosenberg, K. J.; Israelachvili, J. *Proc. Natl. Acad. Sci. U.S.A.* **2006**, *103*, 15739.

(10) (a) Dill, K. A. *Biochemistry* **1990**, *29*, 7133. (b) Tanford, C. *The Hydrophobic Effect: Formation of Micelles and Biological Membranes*; Wiley Interscience: New York, 1980.

(11) Li, C.; Gu, C.; Zhang, Y.; Lang, M. *Polym. Bull.* **2012**, *68*, 69.

(12) Spek, A. L. *Acta Crystallogr., Sect. A: Found. Crystallogr.* **1990**, *46*, 194.

(13) (a) Lu, Z.; Knobler, C. B.; Furukawa, H.; Wang, B.; Liu, G.; Yaghi, O. M. *J. Am. Chem. Soc.* **2009**, *131*, 12532. (b) Furukawa, H.; Kim, J.; Ockwig, N. W.; O'Keeffe, M.; Yaghi, O. M. *J. Am. Chem. Soc.* **2008**, *130*, 11650.

(14) Sing, K. S. W.; Everett, D. H.; Haul, R. A. W.; Moscou, L.; Pierotti, R. A.; Rouquérol, J.; Siemieniewska, T. *Pure Appl. Chem.* **1985**, *57*, 603.